Preprints.org

Article

Not peer-reviewed version

Intranasal Delivery of Cell-Penetrating Therapeutic Peptide Enhances Brain Delivery, Reduces Inflammation, and Improves Neurologic Function in Moderate TBI

Yaswanthi Yanamadala , Ritika Roy , Afrika Williams , Navya Uppu , Audrey Yoonsun Kim , Mark A DeCoster , Paul Kim , Teresa Ann Murray *

Posted Date: 7 May 2024

doi: 10.20944/preprints202405.0360.v1

Keywords: Traumatic brain injury; TBI; secondary injury; peptide therapeutics; cell penetrating peptide; pro-inflammatory cytokines; intranasal drug delivery; blood brain barrier

Preprints.org is a free multidiscipline platform providing preprint service that is dedicated to making early versions of research outputs permanently available and citable. Preprints posted at Preprints.org appear in Web of Science, Crossref, Google Scholar, Scilit, Europe PMC.

Copyright: This is an open access article distributed under the Creative Commons Attribution License which permits unrestricted use, distribution, and reproduction in any medium, provided the original work is properly cited.

Preprints.org (www.preprints.org) | NOT PEER-REVIEWED | Posted: 7 May 2024 doi:10.20944/preprints202405.0360.v1

Disclaimer/Publisher's Note: The statements, opinions, and data contained in all publications are solely those of the individual author(s) and contributor(s) and not of MDPI and/or the editor(s). MDPI and/or the editor(s) disclaim responsibility for any injury to people or property resulting from any ideas, methods, instructions, or products referred to in the content.

Article

Intranasal Delivery of Cell-Penetrating Therapeutic Peptide Enhances Brain Delivery, Reduces Inflammation, and Improves Neurologic Function in Moderate TBI

Yaswanthi Yanamadala[1], Ritika Roy[1], Afrika Williams[1], Navya Uppu[1], Audrey Yoonsun Kim[2], Mark A. DeCoster[1], Paul Kim[2], Teresa Ann Murray[1*]

[1] Center for Biomedical Engineering and Rehabilitation Sciences, Louisiana Tech University, PO Box 10157, Ruston, Louisiana, USA;
[2] Department of Biological Sciences, Grambling State University, Grambling, Louisiana, USA;
* Correspondence: tmurray@latech.edu; 1-318-257-5237

Abstract: Following traumatic brain injury (TBI), secondary brain damage due to chronic inflammation is the most predominant cause of the delayed onset of mood and memory disorders. Currently no therapeutic approach is available to effectively mitigate secondary brain injury after TBI. One reason is the blood-brain barrier (BBB), which prevents passage of most therapeutic agents into the brain. Peptides have been among the leading candidates for CNS therapy due to their low immunogenicity and toxicity, bioavailability, and ease of modification. In this study, we demonstrated that non-invasive intranasal administration of KAFAK, a cell penetrating anti-inflammatory peptide, traversed the BBB in a murine model of diffuse, moderate TBI. Notably, KAFAK treatment reduced the production of pro-inflammatory cytokines that contribute to secondary injury. Furthermore, behavioral tests showed improved or restored neurological, memory, and locomotor performance in KAFAK-treated mice. This study demonstrates KAFAK's ability to cross the blood-brain barrier, to lower pro-inflammatory cytokine levels in vivo, and to restore function after a moderate TBI.

Keywords: traumatic brain injury; TBI; secondary injury; peptide therapeutics; cell penetrating peptide; pro-inflammatory cytokines; intranasal drug delivery; blood brain barrier

1. Introduction

The incidence of CNS diseases such as Alzheimer's disease, traumatic brain injury, brain tumors, and Parkinson's disease have been on the rise for the past few decades [1]. Despite the increased incidence, there are relatively few CNS therapeutics that are currently available [2]. One of the reasons for this is that delivery of many therapeutic molecules to the brain is impeded by the blood-brain barrier (BBB). The brain capillary endothelial cells and the tight junctions between them restrict the transport of macromolecules such as proteins and nucleic acids [3]. Furthermore, most of the newly developed, potent candidates failed in clinical trials owing to the complexity of the barrier [4]. Hence, there is a great need for exploring other means of treating the brain, such as with peptides that can penetrate the BBB.

Peptides have shown great promise as therapeutics due to their favorable properties like lower toxicity, high specificity, increased bioavailability, and scalability of production [5]. Currently, over 70 therapeutic peptides are available, and more are in clinical trials. A few of these peptides have proven their mettle in treating CNS disorders [6,7]. However, most of them have not been evaluated for their ability to cross the BBB.

© 2024 by the author(s). Distributed under a Creative Commons CC BY license.

Preprints.org (www.preprints.org) | NOT PEER-REVIEWED | Posted: 7 May 2024 doi:10.20944/preprints202405.0360.v1

In addition to peptides that directly treat disorders, some peptides are utilized to deliver drugs. Among these are cell-penetrating peptides (CPPs) and receptor-mediated peptides (RMPs). These have shown particularly promising results in facilitating the transport of macromolecules across the BBB [8,9]. CPPs are small cationic or amphipathic peptides that are either endogenous or synthetic [10]. Endogenous peptide carriers offer high efficiency along with minimal cellular toxicity. The ability of some endogenous peptides to shuttle across the BBB has inspired researchers to develop neuropharmaceuticals based on these natural peptides. The exact mechanism of translocation of the CPPs is still debated but they are mostly thought to be transported by adsorptive mediated transcytosis and the translocation is dependent on the cell type and the cargo [11]. CPPs such as TAT protein, SynB, Penetratin, and prion peptides have shown improved therapeutic cargo translocation to the brain compared to therapeutic peptides alone [12]. In contrast, the L57 RMP transcytoses the BBB through LRP1 receptors. We recently demonstrated its improved permeability compared to another RMP, Angiopep-7, in an in vitro BBB model [8].

Traumatic brain injury (TBI) is a complex condition with cell-mediated secondary damage [13] that can lead to chronic neurological disorders months after even a mild injury [14]. The lack of effective diagnostic tools for detecting mild to moderate TBI and the development of secondary damage contribute to the difficulties of TBI management. Secondary damage can be caused by various factors, including inflammatory molecules, reactive oxygen species, and excitotoxicity. Inflammatory cytokines, such as TNF, IL-1β, and IL-6, play a key role in the development of secondary injuries [15,16]. The mitogen-activated protein kinase-activated protein kinase II (MK2) pathway plays a crucial role in neuronal inflammation. Elevated activation of this pathway has been associated with increased levels of TNF, IL-1β, and IL-6, which contribute to secondary damage. KAFAK is an anti-inflammatory CPP that inhibits MK2 [17]. Notably, locally implanted hydrogels containing this therapeutically active CPP and brain-derived neurotrophic factor significantly reduced inflammation in rat spinal cord injury models [18]. Furthermore, KAFAK treatment reduced the expression of pro-inflammatory cytokines TNF, IL-1β, and IL-6 in an ex vivo model of osteoarthritis [18,19].

In this study, primary rat brain microvascular endothelial cells (BMVECs) were utilized to visualize the cellular uptake and localization of three fluorescently labeled peptide drugs: FITC-KAFAK, FITC-L57-AIP-1, and FITC-AIP-1. L57 was conjugated to AIP-1, the therapeutic domain of KAFAK. These peptides were also evaluated for potential cytotoxicity. Primary BMVECs are the first structural cells of the BBB and play a crucial role in regulating the transport of molecules into the brain [20]. The use of primary BMVECs ensures that the experiments closely mimic the conditions of the BBB in vivo. KAFAK exhibited significantly better uptake compared to L57-AIP-1 and AIP-1 alone, even at low concentrations. Furthermore, KAFAK therapy using clinically relevant intranasal infusion, conferred protective effects on behavior in a midline fluid percussion model of TBI mice. It also reduced inflammatory cytokine levels in the brain. Due to its ability to cross the BBB via intranasal infusion and to reduce inflammation, KAFAK shows promise as both a drug delivery agent and as a treatment for CNS disorders in which the MK2 pathway is upregulated.

2. Materials and Methods

2.1. Chemicals

The peptides KAFAK-RITC (Rhodamine-B-KAFAKLAARLYRAKLARQLGVAA), KAFAK-FITC (FITC-Ahx-KAFAKLAARLYRAKLARQLGVAA), and L57-AIP-FITC (FITC-AhxTWPKHFDKHTFYSILKLGKH-(Beta-ala)-LARQLGVAA-CONH2) were custom-made and purchased from Biomatik, Canada. The peptide AIP-FITC (FITC-Ahx-KKKALNRQLGVAA) was custom-made and purchased from Aaptec, USA. Ingredients for F12 media mixture (10% horse serum, 10% fetal bovine serum, glutamine, NaHCO3, and heparin) were obtained from ATCC USA and puromycin from Millipore Sigma, St. Louis, MO, USA. Agarose and Tris HCl were purchased from Avantor/VWR. ELISA kits for IL-1β (EK0394) and IL-6 (EK0411) were purchased from Boster Bio and for TNF (BMS607-3) from Thermo Fisher Scientific. The Pierce Rapid Gold BCA protein Assay

Preprints.org (www.preprints.org) | NOT PEER-REVIEWED | Posted: 7 May 2024 doi:10.20944/preprints202405.0360.v1

kit was procured from Thermo Fisher Scientific. Other reagents that were utilized include ketamine hydrochloride (Vedco), 0.9% saline (Teknova), and xylazine (Vet One), polymethyl methacrylate (Lang Dental), low melting point agarose (IBI Scientific), formaldehyde (Ward's Science), monobasic sodium phosphate (MP Biomedicals), dibasic sodium phosphate (Sigma Aldrich), phosphate buffered saline (PBS, Gibco), sucrose (Sigma Aldrich), glycerol (Himedia), n-propyl gallate (MP Biomedicals), and 4',6-diamidino-2-phenylindole, dihydrochloride (DAPI, Roche Diagnostics).

2.2. In Vitro Model

2.2.1. Harvesting Primary Cells

Sprague Dawley rat pups were sacrificed by disarticulation between post-natal days 1-3 and the procedures were carried out following the protocols approved by the Louisiana Tech University Animal Care and Use Committee. Cells were carefully extracted and isolated from the cortex of the pups and cultured in F12 nutrient mixture (10% horse serum, 10% fetal bovine serum, glutamine, NaHCO3, and heparin). The glial cells can differentiate into endothelial cells, astrocytes, and or microglia with specific growth factors and media as previously described [8,21–23]. The glial cells were initially purified by using 5.51 μM puromycin. Next, purified cells were cultured in a rat endothelial growth medium with endothelial growth factors for their differentiation into BMVECs. Early cell passages were used for this study to maintain the characteristics of the BMVECs.

2.2.2. Peptide Uptake and Localization

These cells were seeded onto poly-L-lysine-coated 96-well black-walled plate at 10,000 cells per well. Plates were incubated for 24 hours or until 50%–80% confluent at 37°C in 5% CO2. This was followed by treatment with different concentrations of peptides. All three peptides, FITC-KAFAK, FITC-L57-AIP-1, and FITC-AIP-1, are soluble in PBS. Stock solutions were prepared by dissolving 2 mg/ml of a peptide in 500 μl of PBS. Working concentrations of the peptides (10 μl, 20 μl, 30 μl, 50 μl, 75 μl) were prepared immediately prior to use by diluting the stock concentration in endothelial cell media. Two different passages of cells were used to test each concentration in triplicate. Cells with no peptide treatment were used as controls. The media in the wells was replaced with the corresponding peptide concentration media for the treatment of cells. After treatment, the plate was incubated at 37°C for 4 hours in 5% CO2 incubators. It was then removed from the incubator and washed three times with warm PBS. Gentle washes were performed to prevent losing cells and to maintain the cell membrane integrity. One more wash with PBS was performed after fixing the cells for 10 minutes with paraformaldehyde. To visualize the individual nuclei, cells were stained with DAPI. Epifluorescence images at three random areas of the well were acquired by using consistent image acquisition settings at 10x and 20x magnification in phase contrast, FITC (excitation: 470nm, emission: 530nm), DAPI (excitation: 358nm, emission: 461nm) filters. A Leica DMI 6000B inverted microscope with a Leica DP71 color camera was used for imaging.

ImageJ software was used to quantify fluorescence intensity in images of stained cells. For each well, 20 cells were chosen at random and outlined to determine the mean fluorescence intensity in relative fluorescence units (rfu). The data were corrected by subtracting the mean background fluorescence intensity. Each well's average mean fluorescence intensity was normalized with the mean of the negative control (vehicle treated cells). Rounded cells, which had bright autofluorescence, and undissolved fluorescently labeled peptide aggregates were excluded from the intensity measurements.

2.2.3. ATP Assay

BMVECs were used to evaluate the potential cytotoxicity of peptides at varying concentrations. Endothelial media was used to dilute peptide concentrations from stock to 10 μM, 30 μM, 50 μM, 100 μM, 250 μM, and 500 μM for the three peptides FITC- KAFAK, FITC-L57-AIP, and FITC-AIP-1. Cells (10,000 per well) were seeded on a 96-well plate and treated with each concentration of peptide in triplicate, while three wells served as controls and received no peptide treatment. The plate was

Preprints.org (www.preprints.org) | NOT PEER-REVIEWED | Posted: 7 May 2024 doi:10.20944/preprints202405.0360.v1

incubated for 4 hours at 37°C and 5% CO2 according to the manufacturer's instructions for the ATP assay kit (Promega CellTiter-Glo 1.0). After incubation, the plate was equilibrated for 30 minutes at room temperature, the CellTiter-Glo substrate and buffer were combined, and 100 µl of reagent was added to 100 µl of medium containing cells. The plate was placed on an orbital shaker for two to three minutes to lyse the cells, and a Biotek Cytation imaging reader was used to record the luminescence.

2.3. In Vivo Model

2.3.1. Animal Preparation and Handling

All the experimental procedures, animal care, and handling were carried out according to a protocol approved by the Louisiana Tech University Institutional Animal Care and Use Committee (Protocol 2022-03). Wild-type C57BL/6NHsd mice and Sprague Dawley rats were procured from Jackson laboratory and subsequently bred as needed. The animals were provided with water and food ad libitum and maintained at 12-hour dark/light cycles in a temperature- and humidity-controlled vivarium.

Twelve mice were used for initial experiments to determine the BBB permeability of KAFAK via intraperitoneal and intranasal delivery. They received no injury. Details of the procedure are in the section entitled "Evaluation of BBB permeability."

A total of 24 mice, 8–16 weeks of age, were randomly assigned to the following treatment groups, eight per group with equal numbers of male and female mice per treatment group: 1) Sham TBI with vehicle treatment (Sham); 2) moderate TBI with vehicle treatment (TBI); 3) Administration of KAFAK treatment after TBI (KAFAK). The treatments were administered intranasally (24 µl of 500 µM KAFAK solution) within the first hour after the injury.

To study the anti-inflammatory effect of KAFAK using ELISA, 20 mice were randomly assigned to one of four groups: Sham group (intranasal vehicle treatment), TBI (intranasal vehicle treatment), TBI with intranasally administered KAFAK (24 µl of 500 µM KAFAK), or TBI with intraperitoneal injection of KAFAK (14.6 mg/kg). A power analysis was conducted early in the experiment to determine group sizes.

2.3.2. Intranasal Administration

The mice were weighed and separated into individual cages and allowed time to become acclimated to this condition before being used for the study. They were sedated using 2% isoflurane at 500 ml/min using a SomnoSuite digital vaporizer system (Kent Scientific Corporation, Torrington, CT, USA). They were kept mildly sedated during the treatment with 1% isoflurane while positioned supine at a 70-degree angle. A 6 µl treatment (KAFAK or vehicle) was administered through intranasal infusion, followed by three more treatments at one-minute intervals, into alternating nostrils. Five minutes after infusion, isoflurane administration was stopped, and mice were returned to their home cage and monitored for five minutes before being returned to the vivarium.

2.3.3. Intraperitoneal Administration

The handling of mice for intraperitoneal administration was conducted similarly to that of intranasal administration. KAFAK (14.6 mg/kg) or vehicle was injected into the intraperitoneal sac while the mouse was sedated and laid in the supine position, as described for intranasal infusion. Each mouse was placed into its home cage and monitored for a minimum of five minutes before returning it to the vivarium.

2.3.4. Evaluation of BBB Permeability

Mice received a single treatment of FITC-KAFAK or RITC-KAFAK either intranasally or intraperitoneally to assess the BBB permeability of KAFAK. FITC and RITC labeled KAFAK were used to determine the most effective label for visualizing KAFAK in the brain. Four hours after

Preprints.org (www.preprints.org) | NOT PEER-REVIEWED | Posted: 7 May 2024 doi:10.20944/preprints202405.0360.v1

treatment, each mouse was anesthetized with 2% isoflurane at 500 ml/min (SomnoSuite) to minimize stress before administration of a ketamine/xylazine cocktail (100 mg/kg and 10 mg/kg, respectively), which was administered intraperitoneally. Later, each mouse was returned to its cage to reduce stress. Each mouse was then fixed to a perforated necropsy table in the supine position. While it was deeply anesthetized, an incision was made to expose the thoracic cavity and an incision was made in the right aorta to facilitate blood drainage. Then through the left ventricle, 25 ml of 1X ice-cold PBS was pumped to displace the blood. Once the liver was clear, 4% ice-cold neutral buffered formalin was pumped for fixing the tissue, followed by decapitation and extraction of the brain. The brain was then post-fixed in 4% neutral buffered formalin for eight hours at 4˚C followed by saturation in 30% sucrose overnight and storage at –80˚C.

The frozen brains were sectioned into 60-µm thick coronal slices using an EMS-500 oscillating tissue slicer (Electron Microscopy Sciences) and stored in the dark at 4˚C until slides were prepared. The brain sections were counterstained with DAPI for visualization of cell nuclei. Tissue sections were prepared with gradient concentrations of alcohol before mounting on slides using anti-fade mounting media. Brain sections, including the olfactory bulb, were arranged on slides from rostral to caudal order. The slides were sealed and stored in the dark before being imaged with an Olympus IX51 epifluorescent microscope. To prevent photobleaching of the fluorescent dyes, image acquisition was optimized by minimizing light intensity, acquisition time, and prioritizing FITC/RITC image capture.

2.3.5. Midline Fluid Percussion model of TBI

A midline fluid percussion injury (mFPI) was performed according to our previously published work [13,21]. Briefly, a craniotomy was made at the midline between bregma and lambda and a Luer lock connector was attached to the skull. The connector was filled with sterile saline and sealed with Parafilm. All procedures were conducted under anesthesia. Later that day, a fluid percussion device was used to inject a brief pulse of water that depressed the dura mater causing a moderate diffuse brain injury. The mouse was placed in a supine position and its righting time was recorded. This was one of the metrics used to confirm a moderate TBI. Afterward, the craniotomy was sealed and the mouse was returned to its home cage, and monitored before returning it to the vivarium.

2.3.6. Rotarod Test

The rotarod test was conducted using a Model 76-0770 rotarod system (Panlab) to evaluate vestibulomotor function. To minimize stress the mice were acclimated to the environment for at least 10 minutes and rotarod chambers were thoroughly cleaned between each mouse. Mean time to fall (latency) was recorded to assess the performance of each mouse. On each test day three consecutive trials were conducted with a 10-minute rest time after the second trial. Tests were conducted during the same time of day. The average of the two best scores was recorded for each day. For three days prior to injury and treatment, mice were trained at a consistent time of the day (–3, –2, –1 day prior to injury). The mean score from Day –1 was used as the baseline score for normalizing the latencies for tests on the second, fifth and seventh day after injury (Day 2, Day 5, and Day 7, respectively). Tests on Days 2, 5, and 7 were conducted at the same time of day as the training trials. Scores for Days 2, 5, and 7 were normalized to each animal's baseline score to minimize variability.

2.3.7. Modified Neurological Severity Score (mNSS)

This series of tests was conducted to assess the impairments in reflexes, balance, vision, and tactile sensory functions. To evaluate these impairments, the following eight tests were conducted: hindlimb flexion, startle response (a sudden clap of the hands), seeking behavior, the ability to walk on elevated bars 3 cm, 2 cm, and 1 cm wide and 30 cm long, and the ability to balance on a 0.5-cm wide square beam for at least 30 seconds, and the time that the mouse balanced on a 0.5-cm thick circular rod. Failure in each task added one point to the mNSS results. A score of zero indicates

Preprints.org (www.preprints.org) | NOT PEER-REVIEWED | Posted: 7 May 2024 doi:10.20944/preprints202405.0360.v1

normal function and higher scores scale with the severity of the brain injury and neurological dysfunction.

2.3.8. Novel Object Recognition (NOR)

This test was conducted to compare memory function between treatment groups. The NOR test is based on a rodent's natural tendency to explore novel objects. It was performed under low stress conditions, after 5 minutes of acclimation to the open box. In addition, the box was thoroughly cleaned between each mouse. To start the test, a mouse was placed in the center with two identical sized objects in the opposite corners of the box. Their exploration of the objects was recorded for 5 minutes. Subsequently, the recording was continued for another 5 minutes after one of the objects was replaced with a different shaped object (novel object). Video recordings of each test were analyzed using MATSAP software [24] to quantify the time spent exploring the novel object. The discrimination index (DI) was calculated as DI = (time spent with new object multiplied by 100) / (time spent with original object plus the time spent with the novel object).

Videos of NOR behavioral tests were converted to Audio Video Interleave (AVI) files at ten frames per second. The audio in the files were deleted and then uncompressed and converted to gray scale using the same software. The videos were trimmed to 300 seconds (5 minutes) and the last frame was edited to remove the mouse from the frame. This edited frame was used as a background for the video [24]. If needed, the frames were cropped to square, removing the background, to exactly fit the video to the open box. After necessary edits the files were converted to multi-TIFF files that were read by plugins.

2.3.9. Cytokine Analysis

To assess the ability of KAFAK to reduce proinflammatory cytokine production, mice received KAFAK intranasally (24 µl of 500 µM KAFAK) or intraperitoneally (16.4 mg/kg) within the first one hour after a mFPI. The mice were anesthetized 12 hours after treatment and perfused as described in the section entitled Evaluation of BBB permeability. Brains were extracted, weighed, and homogenized using a tissue homogenizer with lysis buffer cocktail (500 µl per hemisphere). To avoid cytokine degradation, brains were handled in cold conditions from the time they were extracted. After homogenization, the mixture was sonicated and then placed on an orbital shaker for 15 minutes at 4°C followed by centrifugation at 19,000 x g. The supernatant was collected and stored at –80°C until ELISA was performed. For ELISA, samples were thawed on ice, protein concentrations were quantified by BCA assay then diluted with lysis buffer to ensure that the measurements fell within the working range of the kits, and the ELISA was performed according to the manufacturer's protocols.

2.3.10. Statistical Analysis

SPPS software version 28.0.1.0 was used for statistical analysis for behavioral tests and Gpower version 3.1.9.7 was used for the calculation of the statistical power. The Bonferroni correction was used to adjust for all multiple comparisons during statistical hypothesis testing.

3. Results

3.1. In Vitro Model

3.1.1. Internalization of Fluorescently Labelled Peptides by Brain Microvascular Endothelial Cells

To compare the internalization efficiency of KAFAK, L57-AIP-1, and AIP-1 in primary BMVECs, the peptides were fluorescently tagged and visualized 4 hours after treatment with varying concentrations of the peptide. Even at low concentrations, FITC-KAFAK and FITC-L57-AIP-1 were readily internalized by the BMVECs within the first few minutes after the treatment. Both exhibited diffuse staining in the cells (Figure S1, Supplemental Data). The intensity, in rfu, of FITC-KAFAK was

Preprints.org (www.preprints.org) | NOT PEER-REVIEWED | Posted: 7 May 2024 doi:10.20944/preprints202405.0360.v1

much higher compared to the FITC-L57-AIP (Figure 1). However, FITC-AIP-1 alone did not exhibit any internalization, even at the 100 μM level. While increasing the light intensity showed substantial FITC-L57-AIP-1 internalization at 20 μM we maintained a lower, consistent intensity level for all peptides across all concentrations. The concentrations of FITC-KAFAK beyond 75 μM were also measured, but the fluorescence intensity was too great to acquire unsaturated images, therefore they are not included in the figure.

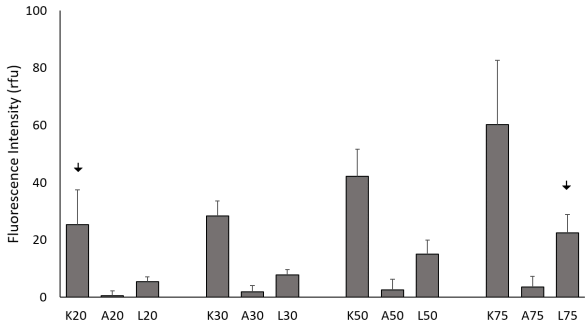

Figure 1. Concentration-dependent uptake of fluorescently labeled peptides. Fluorescently labeled peptides at various concentrations were incubated with BMVECs (10,000 per well) for 4 hours with 20, 30, 50, and 75 μM of FITC-KAFAK (K20 – K75), FITC-AIP-1 (A20 – A75), and FITC-L57-AIP-1 (L20 – L75). All three peptides exhibited concentration-dependent cellular uptake. However, intensity of internalized FITC-AIP-1 was significantly lower for all concentrations ($p<0.01$). Even the highest concentration of FITC-AIP-1 had a significantly lower fluorescence intensity than the lowest concentration of KAFAK (A75 vs K20, $p<0.01$). Whereas the intensity for FITC-L57-AIP-1 was higher than FITC-AIP-1 for each concentration level ($p<0.01$), it was also significantly lower than concentration of FITC-KAFAK at each concentration level ($p<0.01$). However, 75 μM FITC-L57-AIP-1 produced about the same fluorescence as 20 μM of KAFAK (downward arrows in figure). ImageJ software was used to analyze 20 cells per well, for a total of 120 cells (n=6 wells) per concentration of a peptide. Mean fluorescence intensity was normalized to control cells with no peptide and the relative fluorescence intensity was analyzed using ANOVA with a Bonferroni correction for multiple comparisons (data are represented as mean ± 2 standard deviations in figure).

3.1.2. Comparison of Peptide Uptake

Internalization of all three peptides was concentration dependent (Figure 1). FITC-KAFAK had a much greater level of internalization at all concentrations (Figure S1, Supplementary Data) than the other two peptides with only one exception; 20 μM FITC-KAFAK was similar to the uptake of 75 μM of FITC-L57-AIP-1. Thus, the highest concentration of FITC-L57-AIP-1 tested had a similar level of uptake to the lowest concentration of KAFAK ($p>0.05$). Both FITC-L57-AIP-1 and FITC-KAFAK had significantly greater uptake compared to FITC-AIP-1 at all concentrations. FITC-L57-AIP-1, a receptor-mediated peptide (RMP), was successfully internalized; however, its uptake was modest compared to FITC-KAFAK, a CPP peptide. FITC-AIP-1 (the therapeutic peptide in FITC-KAFAK), which is not a CCP or RMP, was only marginally taken up by the cells at higher concentrations.

3.1.3. Viability of BMVEC with Peptide Treatment

Cell viability was assessed using an ATP assay after 24 hours of treatment with three peptides at varied concentrations. FITC-L57-AIP-1 and FITC-AIP-1 exhibited no cytotoxic effects at concentrations up to 500 μM (Figure 2). FITC-KAFAK treatment resulted in a concentration-dependent decrease in BMVEC viability, with a significant reduction to 70% starting at 250 μM.

Preprints.org (www.preprints.org) | NOT PEER-REVIEWED | Posted: 7 May 2024 doi:10.20944/preprints202405.0360.v1

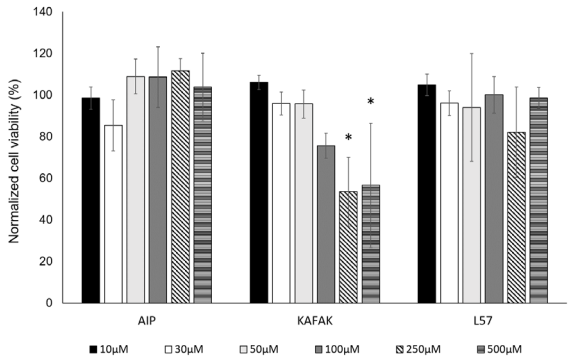

Figure 2. An ATP assay was used to measure cell viability in BMVECs with the indicated concentrations of peptide after 24 hours of incubation. FITC-AIP-1 (AIP) and FITC-L57-AIP-1 (L57) and did not elicit cytotoxicity between 10–500 μM. KAFAK treatment from 10 to 100 μM did not significantly affect cell viability, with some reduction of cell viability at 250–500 μM. Data are expressed as % of control (mean ± SD, n=3 wells/concentration of each peptide *p<0.05).

3.2. In Vitro Model

3.2.1. Visualization of KAFAK Noninvasively Delivered to the Brain

To investigate the biodistribution of KAFAK in the brain and optimize the dose and route of delivery of the peptide, we used a murine model. FITC-KAFAK was administered either intranasally or intraperitoneally. FITC-KAFAK was not observed in the brain after intraperitoneal administration. In contrast, it was observed in the olfactory bulb upon intranasal administration. However, no fluorescence was detected in more caudal regions. Furthermore, we encountered bleaching challenges with the FITC dye. After replacing the FITC label with Rhodamine (RITC), we observed a greater intensity of the labeled peptide across all regions of the brain as seen in Figure 3. Fluorescence intensity was greater in rostral regions of the brain compared to caudal regions. This suggests not only subarachnoid space diffusion but also parenchymal uptake of KAFAK.

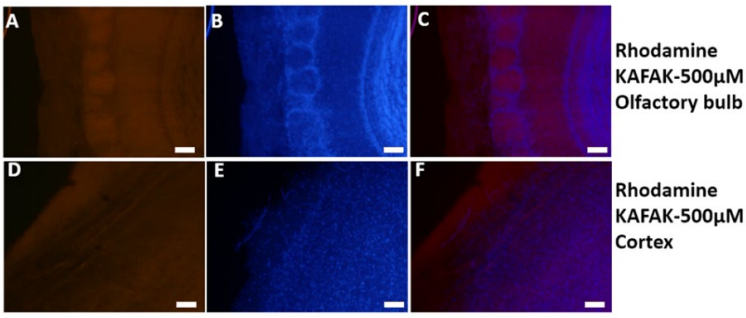

Figure 3. Intranasal delivery of KAFAK to the brain. Mice were treated with 500 μM RITC-KAFAK. Mice were perfused four hours after treatment and brain sections were stained with DAPI. Images A-F are of two representative sections showing that FITC-KAFAK (A) and RITC-KAFAK (B) permeated the olfactory bulb. Images G-I are of a representative section from the cerebral cortex. Images in the first column show fluorescently labeled KAFAK in the olfactory bulb and cortex, as labeled, with DAPI counterstaining shown in the second column. The KAFAK and DAPI images are merged in the third column. Scale bar is 100 μm.

3.2.2. Performance in Rotarod Test after TBI Improves with KAFAK Treatment

Rotarod tests were conducted to assess vestibulomotor coordination. The latency to fall for each mouse was normalized to its baseline latency. As expected, both the TBI-vehicle and TBI-KAFAK groups had reduced mean latency to fall on Day 2 compared to the Sham-vehicle group which confirmed their impaired motor coordination after a moderate TBI. However, by Day 5, the mean

Preprints.org (www.preprints.org) | NOT PEER-REVIEWED | Posted: 7 May 2024 doi:10.20944/preprints202405.0360.v1

normalized latency of the KAFAK-treated group was the same as the mean performance of the Sham group. The latency of the TBI-vehicle group remained significantly lower than that of Sham and KAFAK-treated groups. On Day 7, even though non-significant, the KAFAK-treated mice improved motor skills compared to the TBI-mice group, as depicted in Figure 4. This suggests a potential positive effect of KAFAK on motor function recovery following TBI. KAFAK-treated male mice have shown increased latency scores compared to the sham group which is not observed in the female group (see Figure 4B and 4C). There may be a sex-specific effect of KAFAK, but further investigation is needed due to the small sample size.

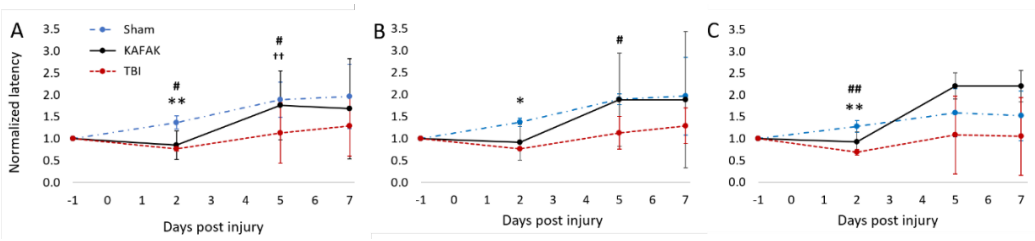

Figure 4. Mean normalized rotarod scores on Day 2, 5 and 7 for TBI-vehicle (TBI), Sham-vehicle (Sham) and TBI-KAFAK (KAFAK) groups. (A) shows the performance for all mice, while (B) and (C) represent the performance of female and male mice, respectively. (Mean ± SD, n = 8 for each group in A and n = 4 for each group in B and C; * $p < 0.05$ Sham versus KAFAK and TBI, ** $p < 0.01$ Sham versus KAFAK and TBI, # $p < 0.05$ TBI versus KAFAK, ## $p < 0.01$ TBI versus KAFAK, †† $p < 0.01$ Sham versus TBI).

3.2.3. KAFAK Treatment Improves Neurological Function in TBI Mice

The neuroprotective effect of the KAFAK peptide after TBI in mouse was evaluated with the mNSS test. The KAFAK-treated and the TBI-vehicle groups had similar results on Day 2, potentially due to a delayed effect of KAFAK. However, by Day 5 KAFAK treated animals, irrespective of gender, had significantly improved performance versus the TBI-vehicle group (Figure 5), and no significant difference compared to the Sham group indicating rescue of neurological function.

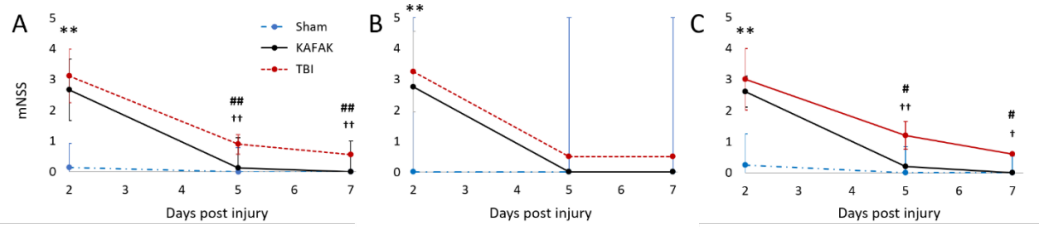

Figure 5. Mean mNSS for TBI-vehicle (TBI), Sham-vehicle (Sham), and TBI-KAFAK (KAFAK) treated groups on Day 2, 5 and 7 (days after injury). Plots show mNSS results for (A) all mice, (B) female mice, and (C) male mice. (Data are expressed as the mean ± SD, n = 8 for each group in A and n = 4 for each group in B and C; ** $p < 0.01$ Sham versus KAFAK and TBI, # $p < 0.05$ TBI versus KAFAK, ## $p < 0.01$ TBI versus KAFAK, † $p < 0.05$ Sham versus TBI, †† $p < 0.01$ Sham versus TBI).

3.2.4. KAFAK Restores Memory Test Performance in TBI Mice

A novel object recognition (NOR) test was conducted to determine whether KAFAK rescues memory deficits caused by TBI. KAFAK treated mice had a significantly higher discrimination index (Figure 6) indicating their ability to identify and distinguish between novel and familiar objects, which was relatively poor for the TBI-vehicle treated group. Furthermore, the KAFAK treated mice had statistically similar results to Sham animals which suggests that KAFAK rescued memory impairments.

Preprints.org (www.preprints.org) | NOT PEER-REVIEWED | Posted: 7 May 2024 doi:10.20944/preprints202405.0360.v1

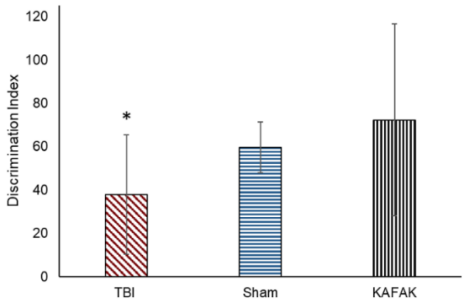

Figure 6. KAFAK treatment rescued memory deficits associated with TBI. The mean discrimination index in novel object recognition test results for the TBI-vehicle group (TBI) was significantly lower than both Sham-vehicle (Sham) and TBI-KAFAK treated (KAFAK) groups seven days after injury (n=8/group, mean of the discrimination index ± 2SD, * p<0.01 for TBI versus KAFAK and for TBI versus Sham).

3.2.5. KAFAK Peptide Reduces the Pro-Inflammatory Cytokine Production in TBI Mice

Cytokine assays were conducted to assess the therapeutic efficiency of KAFAK peptide to suppress elevated levels of inflammatory cytokines that are part of the secondary injury cascade after a moderate TBI. Four groups were tested, including Sham-vehicle (Sham), TBI-vehicle (TBI), KAFAK administered intranasally (KAFAK IN) and KAFAK administered intraperitoneally (KAFAK IP). Initially three mice were evaluated in each group, and upon completing a power analysis, two more were added to each group. Intranasal administration resulted in a greater reduction of all three pro-inflammatory cytokines which included tumor necrosis factor (TNF), interluekin-1 beta (IL-1β), and IL-6. Overall, intraperitoneal administration had a less pronounced effect in reducing the cytokines compared to intranasal administration (Figure 7). The Sham group and intranasally administered KAFAK treated group were statistically similar, while the other two groups had significantly higher levels of these cytokines. These data suggest that intranasal administration of KAFAK can restore normal levels of these cytokines.

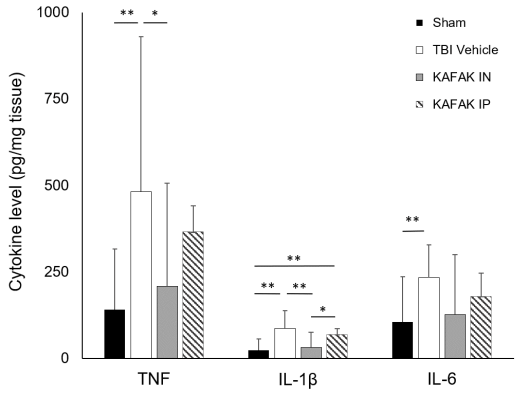

Figure 7. Intranasal administration of KAFAK (KAFAK IN) after TBI reduced levels of key pro-inflammatory cytokines, TNF, IL-1β and IL-6, to sham levels. ELISA results show a significant increase in these cytokines in vehicle-treated mice (TBI Vehicle) versus Sham-injured, vehicle treated mice (Sham). A significant reduction of TNF and IL-1β was observed in the KAFAK IN group versus the TBI Vehicle group. In contrast, no difference was observed between the TBI Vehicle group and the group that received an intraperitoneal delivery of KAFAK (KAFAK IP). (mean pg/mg tissue ± 2SD, n=5/group, * p<0.05, **p<0.01).

4. Discussion

The anti-inflammatory effects of KAFAK have been reported in scientific literature in an osteoarthritis model [19]. Notably, it exhibits superior cell-penetrating ability and less toxicity

Preprints.org (www.preprints.org) | NOT PEER-REVIEWED | Posted: 7 May 2024 doi:10.20944/preprints202405.0360.v1

compared to other CPPs. KAFAK's potential in treating various disorders in vivo, was demonstrated in a spinal cord injury model, and it has shown promise as an anti-inflammatory agent 18. However, its ability to permeate the BBB and its suitability to treat traumatic brain injury using a non-invasive, clinically relevant route of administration remained unclear. This possibility was the motivation for the present study.

In our previous study, L57, an RMP, demonstrated enhanced permeability in an in vitro model of the BBB using primary BMVECs compared to another receptor-mediated peptide Angiopep-7 [8]. In this study, we compared the permeability of L57 conjugated to an anti-inflammatory peptide AIP-1 (L57-AIP-1) to the CPP-therapeutic peptide, KAFAK in the same in vitro BBB model as our previous study. Our results showed enhanced permeability of KAFAK compared to the L57-AIP-1 conjugate, and to the AIP-1 peptide alone. The L57 peptide is internalized via LRP-1 receptors which are highly expressed in disease conditions [25,26]. The L57-AIP-1 and AIP-1 elicited less toxicity compared to the CPP, KAFAK. The low level of uptake of AIP-1, our negative control, was expected as this peptide is neither a CPP nor an RMP. The cytotoxicity of KAFAK at very high concentrations is likely attributed to the higher uptake of KAFAK. We found that low concentrations of KAFAK resulted in higher internalization than higher concentrations of L57-AIP-1 and much higher concentrations of AIP-1. Thus, a low concentration of KAFAK may be all that is required for clinical use. Earlier work supports this notion as KAFAK showed improved therapeutic effect in hepatocytes at lower concentrations compared to the AIP-1 [27].

Using an in vivo model, our results revealed that the noninvasive IN administration of fluorescently labeled KAFAK, at a minimal dose, resulted in a diffuse distribution of the peptide across the brain parenchyma, as observed through fluorescence imaging. In contrast, IP administration resulted in a lower fluorescence intensity, implying that this route of administration is not as effective to deliver KAFAK to the brain.

Non-invasive intranasal administration KAFAK resulted in improved behavior after a moderate, diffuse brain injury in mice versus injured mice treated with the vehicle only. Improvements in vestibular motor skills, neurological function, and memory were observed. Thus, KAFAK treatment had a broad range of effects which suggests a widespread reduction of inflammation. Future work will investigate levels of inflammation in specific brain regions to confirm this.

The cytokines TNF, IL-1β, and IL-6 are among TBI biomarkers that are involved in secondary injury. In our study, we evaluated whether the KAFAK peptide would reduce the levels of these pro-inflammatory cytokines when administered shortly after induction of a diffuse TBI. IN administration of KAFAK resulted in significantly decreased levels of pro-inflammatory cytokines to Sham levels. In contrast, IP administration did not result in significantly lower cytokine levels versus vehicle-treated mice, suggesting that IN administration is more effective than IP delivery. The MK2 pathway is strongly involved with the production of these cytokines [28], and KAFAK acts by inhibiting this process [17]. The reduction of these proinflammatory cytokines may be due to the suppression of MK2 pathway in the brain.

In conclusion, this is the first study to demonstrate in vivo BBB permeability of the KAFAK peptide, to our knowledge. Further, we showed that the peptide improved behavioral performance post-TBI and reduced the production of pro-inflammatory cytokines that are involved in secondary injury. Future studies will explore the synergetic effect of KAFAK in combination with other anti-inflammatory drugs and neuroprotective agents. Although we observed non-significant sex-related differences in behavior, further investigation is warranted, including potential sex differences for dosage levels, toxicity, and pharmacokinetics.

Supplementary Materials: The following supporting information can be downloaded at the website of this paper posted on Preprints.org.

Author Contributions: Conceptualization and methodology, Y.Y., M.A.D., P.K., and T.A.M. Investigation, Y.Y., R.R., A.Y.K., and N.U. Formal analysis, A.W., Y.Y., and T.A.M. Supervision, T.A.M., P.K., M.A.D. Writing – original draft, Y.Y., R.R., A.W., P.K., T.A.M. All authors have read and agreed to the published version of the manuscript.

Preprints.org (www.preprints.org) | NOT PEER-REVIEWED | Posted: 7 May 2024 doi:10.20944/preprints202405.0360.v1

Funding: This work was funded, in part, by the Herman A. "Dusty" Rhodes Eminent Scholar Chair in Engineering which is made available through the State of Louisiana Board of Regents Funds and the National Institutes of Health (Award NS114723) to T.AM. Funding was also provided by a grant from the National Science Foundation Implementation Project (Award 1818697) to Grambling State University. Support was also provided by The James E. Wyche III Endowed Professorship which is made available through the Louisiana Board of Regents Funds to M.A.D. A.W. was supported by a doctoral fellowship from the Louisiana Board of Regents.

Institutional Review Board Statement: The animal study protocol was approved by the Institutional Animal Care and Use Committee of Louisiana Tech University (Protocol 2022-03 approved April 20, 2022).

Informed Consent Statement: Not applicable; no human subjects.

Data Availability Statement: Data are available at https://figshare.com/account/home#/projects/202962.

Conflicts of Interest: The authors declare no conflicts of interest. The funders had no role in the design of the study; in the collection, analyses, or interpretation of data; in the writing of the manuscript; or in the decision to publish the results.

References

1. Feigin, V. L. et al. Global, regional, and national burden of neurological disorders, 1990–2016: a systematic analysis for the Global Burden of Disease Study 2016. Lancet. Neurol. 18, 459 (2019). https://doi.org/10.1016/s1474-4422(18)30499-x
2. Srikanth, M. & Kessler, J. A. Nanotechnology—novel therapeutics for CNS disorders. Nat. Rev. Neurol. 8, 307 (2012). https://doi.org/10.1038/nrneurol.2012.76
3. Stamatovic, S. M., Keep, R. F. & Andjelkovic, A. V. Brain Endothelial Cell-Cell Junctions: How to "Open" the Blood Brain Barrier. Curr. Neuropharmacol. 6, 179 (2008). https://doi.org/10.2174%2F157015908785777210
4. Cummings, J. Lessons Learned from Alzheimer Disease: Clinical Trials with Negative Outcomes. Clin. Transl. Sci. 11, 147–152 (2018). https://doi.org/10.1111/cts.12491
5. Gupta, S. et al. In silico approach for predicting toxicity of peptides and proteins. PLoS One 8, (2013). https://doi.org/10.1371/journal.pone.0073957
6. Kumar, P. et al. Transvascular delivery of small interfering RNA to the central nervous system. Nat. 2007 4487149 448, 39–43 (2007). https://doi.org/10.1038/nature05901
7. Lee, J. H., Zhang, A., You, S. S. & Lieber, C. M. Spontaneous Internalization of Cell Penetrating Peptide-Modified Nanowires into Primary Neurons. Nano Lett. 16, 1509–1513 (2016). https://doi.org/10.1021/acs.nanolett.6b00020
8. Rodrigues J.P., Prajapati, N., DeCoster, M.A., Poh, S., & Murray, T.A. Efficient LRP1-Mediated Uptake and Low Cytotoxicity of Peptide L57 In Vitro Shows Its Promise as CNS Drug Delivery Vector. J. Pharm. Sci. 110, 824–832 (2021). https://doi.org/10.1016%2Fj.xphs.2020.09.019
9. Gitton, Y., Tibaldi, L., Dupont, E., Levi, G. & Joliot, A. Efficient CPP-mediated Cre protein delivery to developing and adult CNS tissues. BMC Biotechnol. 9, (2009). https://doi.org/10.1186/1472-6750-9-40
10. Sibrian-Vazquez, M., Jensen, T. J. & Vicente, M. G. H. Synthesis, characterization, and metabolic stability of porphyrin-peptide conjugates bearing bifunctional signaling sequences. J. Med. Chem. 51, 2915–2923 (2008). https://doi.org/10.1021/jm701050j
11. Zorko, M. & Langel, Ü. Cell-penetrating peptides: mechanism and kinetics of cargo delivery. Adv. Drug Deliv. Rev. 57, 529–545 (2005). https://doi.org/10.1016/j.addr.2004.10.010
12. Zou, L.-L., Ma, J.-L., Wang, T., Yang, T.-B. & Liu, C.-B. Cell-Penetrating Peptide-Mediated Therapeutic Molecule Delivery into the Central Nervous System. Curr. Neuropharmacol. 11, 197 (2013). https://doi.org/10.2174%2F1570159X11311020006
13. Pernici, C. D. et al. Longitudinal optical imaging technique to visualize progressive axonal damage after brain injury in mice reveals responses to different minocycline treatments. Sci. Reports 2020 101 10, 1–16 (2020). https://doi.org/10.1038/s41598-020-64783-x
14. Flygt, J., Djupsjö, A., Lenne, F. & Marklund, N. Myelin loss and oligodendrocyte pathology in white matter tracts following traumatic brain injury in the rat. Eur. J. Neurosci. 38, 2153–2165 (2013). https://doi.org/10.1111/ejn.12179
15. Lu, K. T., Wang, Y. W., Yang, J. T., Yang, Y. L. & Chen, H. I. Effect of Interleukin-1 on Traumatic Brain Injury–Induced Damage to Hippocampal Neurons. https://home.liebertpub.com/neu 22, 885–895 (2005). https://doi.org/10.1089/neu.2005.22.885
16. Ferreira, L. C. B. et al. Increased levels of interleukin-6, -8 and -10 are associated with fatal outcome following severe traumatic brain injury. Brain Inj. 28, 1311–1316 (2014).
17. Bartlett, R. L., Sharma, S. & Panitch, A. Cell-penetrating peptides released from thermosensitive nanoparticles suppress pro-inflammatory cytokine response by specifically targeting inflamed cartilage

Preprints.org (www.preprints.org) | NOT PEER-REVIEWED | Posted: 7 May 2024 doi:10.20944/preprints202405.0360.v1

explants. Nanomedicine Nanotechnology, Biol. Med. 9, 419–427 (2013). https://doi.org/10.1016/j.nano.2012.09.003
18. He, Z. et al. An anti-inflammatory peptide and brain-derived neurotrophic factor-modified hyaluronan-methylcellulose hydrogel promotes nerve regeneration in rats with spinal cord injury. Int. J. Nanomedicine 14, 721 (2019). https://doi.org/10.2147/ijn.s187854
19. McMasters, J., Poh, S., Lin, J. B. & Panitch, A. Delivery of anti-inflammatory peptides from hollow PEGylated poly(NIPAM) nanoparticles reduces inflammation in an ex vivo osteoarthritis model. J. Control. Release 258, 161–170 (2017). https://doi.org/10.1016/j.jconrel.2017.05.008
20. Navone, S. E. et al. Human and mouse brain-derived endothelial cells require high levels of growth factors medium for their isolation, in vitro maintenance and survival. Vasc. Cell 5, 1–12 (2013). https://doi.org/10.1186/2045-824x-5-10
21. Karekar, N. et al. Self-Assembled Metal-Organic Biohybrids (MOBs) Using Copper and Silver for Cell Studies. Nanomater. (Basel, Switzerland) 9, (2019). https://doi.org/10.3390/nano9091282
22. Abbott, N. J., Hughes, C. C. W., Revest, P. A. & Greenwood, J. Development and characterisation of a rat brain capillary endothelial culture: towards an in vitro blood-brain barrier. J. Cell Sci. 103 (Pt 1), 23–37 (1992). https://doi.org/10.1242/jcs.103.1.23
23. Scoggin, J. L. et al. An enzyme-based electrochemical biosensor probe with sensitivity to detect astrocytic versus glioma uptake of glutamate in real time in vitro. Biosens. Bioelectron. 126, 751–757 (2019). https://doi.org/10.1016/j.bios.2018.11.023
24. Holly, K. S., Orndorff, C. O. & Murray, T. A. MATSAP: An automated analysis of stretch-Attend posture in rodent behavioral experiments. Sci. Rep. 6, (2016). https://doi.org/10.1038%2Fsrep31286
25. Qiu, Z., Strickland, D. K., Hyman, B. T. & Rebeck, G. W. Elevation of LDL receptor-related protein levels via ligand interactions in Alzheimer disease and in vitro. J. Neuropathol. Exp. Neurol. 60, 430–440 (2001). https://doi.org/10.1093/jnen/60.5.430
26. Pires, L. A. et al. Effect of neoadjuvant chemotherapy on low-density lipoprotein (LDL) receptor and LDL receptor-related protein 1 (LRP-1) receptor in locally advanced breast cancer. Brazilian J. Med. Biol. Res. = Rev. Bras. Pesqui. medicas e Biol. 45, 557–564 (2012). https://doi.org/10.1590/s0100-879x2012007500068
27. Kim, P. et al. Cell-Penetrating MK2 Inhibitory Peptide Blocks LPS-Induced Expression of Proinflammatory Cytokines in HepG2 Hepatocytes. FASEB J. 34, 1–1 (2020). https://doi.org/10.1096/fasebj.2020.34.s1.09121
28. Qeadan, F., Bansal, P., Hanson, J. A. & Beswick, E. J. The MK2 pathway is linked to G-CSF, cytokine production and metastasis in gastric cancer: A novel intercorrelation analysis approach. J. Transl. Med. 18, 1–13 (2020). https://doi.org/10.1186/s12967-020-02294-z

Disclaimer/Publisher's Note: The statements, opinions and data contained in all publications are solely those of the individual author(s) and contributor(s) and not of MDPI and/or the editor(s). MDPI and/or the editor(s) disclaim responsibility for any injury to people or property resulting from any ideas, methods, instructions or products referred to in the content.